

Geomorphometric Analysis of Karst Terrains

Eulogio Pardo-Igúzquiza, Juan José Durán, Juan Antonio Luque-Espinar and Pedro Robledo-Ardila

Abstract

The availability of high-resolution digital elevation models (DEM) has increased the possibilities of geomorphometric analysis of karst terrains. Apart from the classical terrain parameters (distribution of elevations, slopes, orientations, curvature, etc.), there have been developments of new algorithms that expand further the possibilities of numerical terrain analysis. We present the analysis of the three main features of the karst landscape: the topographic surface, karst hills and karst depressions. Karst depressions and karst hills have been identified and delineated using the DEM and field work. We have developed a system of spatial kernel functions that allows to analyze both the relief and karst depressions and hills. The results will be compared with the main conditioning factors in the development of a karst landscape: geology (lithology and structure) and the system of discontinuities and fractures (faults, joints, etc.). We apply the methodology to the Sierra de las Nieves karst massif, and we conclude how a strong structural control has modeled the landscape.

2.1	Introduction – 22
2.2	Methodology – 22
2.3	Case Study – 24
2.4	Conclusions – 25
	References – 26

2.1 Introduction

The quantitative study of the karst landscapes (i.e., the exokarst) has improved significantly during the last decades because the availability of high-resolution digital elevation models (DEMs). In Spain, the *Instituto Geográfico Nacional* offers a DEM with a square cell size of 5 m length on a side. That DEM is public domain and covers the whole of Spain. These digital “topographic maps” are especially suited for quantitative analysis. It is well known that, in the past, the elaboration of a slope map took weeks of man work. Nowadays to draw the same map using a DEM and a computer takes only a few seconds. The same can be said for many parameters (slope orientation, curvature, texture, fractal dimension, local semi-variogram, etc.) that have been incorporated in the spatial analysis toolbox of many geographic information systems. It is obvious that the resolution of the DEM imposes a limit to the scale of the landscape features that can be analyzed. Thus, by using a DEM with a cell of 5 m × 5 m, it is impossible to analyze the karren with centimetric scale or karst depressions that are much smaller than the size of a cell. Nevertheless, the quantitative analysis of DEM with 5 m × 5 m offers a large number of possibilities to analyze the features of the landscape that are larger than the cell size. Thus, karst depressions and karst hills and discontinuities of the karst landscape (any kind of scarp) can be efficiently studied by numerical algorithms that are applied to the DEM. In this work, we propose a method of spatial adaptive kernels in order to identify “principal directions” in the karst terrain, in karst depressions and in karst hills. For karst depressions, these principal directions in the depressions correspond to main directions of development and growth (i.e., preferential directions of dissolution on the plane). For hills, the principal directions are also main directions of development. Finally for the karst relief itself, the principal directions are related to the structural disposition of the layer of rocks and to faults and fractures that produce scarps. In the next section, we introduce the methodology used in this work. In a subsequent section, the methodology is applied to the karst massif of Sierra de las Nieves in the province of Málaga in southern Spain.

2.2 Methodology

A DEM in raster format is a matrix of numbers where each number represents the mean altitude of a cell of terrain with dimensions given by the DEM resolution. This mathematical structure is very adequate for quantitative analysis using numerical algorithms. This has expanded

the possibilities of geomorphometric analysis of any terrain and particularly karst terrains. For example, the calculation of the hypsometric curve (Strahler and Strahler 1992) for a given region is a question of seconds (Bishop and Shroder 2004), while in the past it required too much effort. However, quantitative terrain analysis from DEMs has expanded the possibilities of deriving more elaborated parameters, functions and indexes. In this sense, Pardo-Igúzquiza et al. (2013) proposed a method for the identification and delineation of karst depressions from the DEM. The result is a census of karst depressions with a high-resolution bathymetric map of the depressions. As an example, Fig. 2.1 shows the DEM of the study area and one of the identified depressions has been represented in Fig. 2.2.

The extension of the methodology of karst depressions for mapping karst hills has been shown in Pardo-Igúzquiza et al. (2014). Figure 2.3 shows the karst hills of the central part of the Sierra de las Nieves. Furthermore, apart the depressions, the other aspect of the karst landscape that is going to be analyzed by spatial adaptive kernels are the karst scarps of the landscape as visualized in Fig. 2.4.

The spatial adaptive kernels are defined by a function $k(s)$ that has some desirable mathematical properties (Shimazaki and Shinomoto 2010):

- The kernel satisfies a normalization condition:

$$\int k(s)ds = 1 \quad (2.1)$$

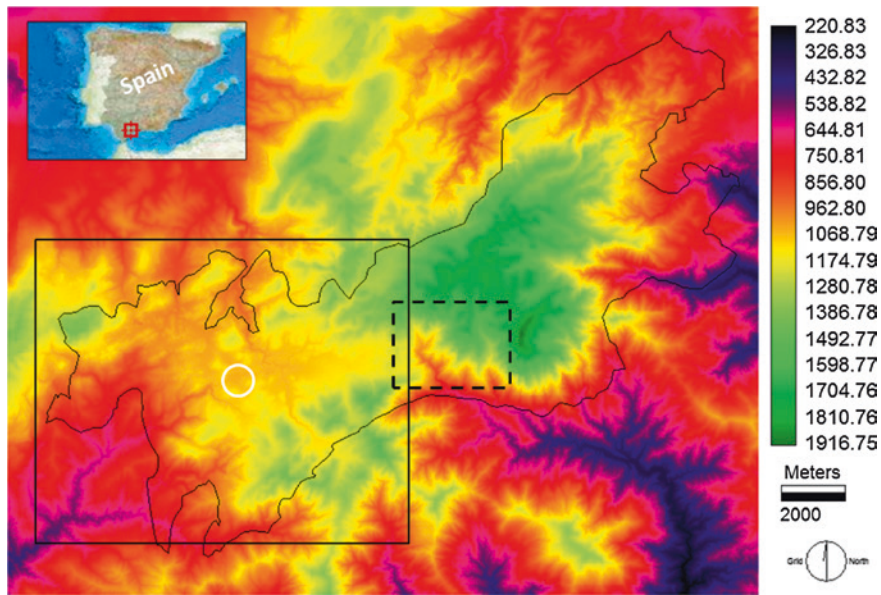
- The kernel has a zero first moment:

$$\int sk(s)ds = 0 \quad (2.2)$$

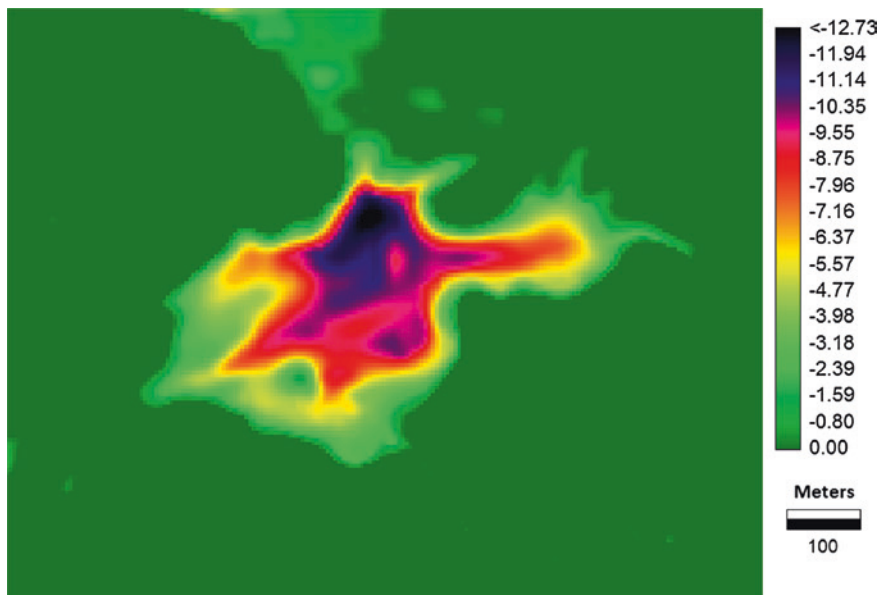
- The kernel has a finite bandwidth:

$$\int s^2 k(s)ds < \infty \quad (2.3)$$

One of the functions with those properties and whose bandwidth is easy to calibrate is the Gauss density function. A bivariate Gaussian kernel is shown in Fig. 2.5 for two different bandwidths with the bandwidth in Fig. 2.5a being shorter than the bandwidth in Fig. 2.5b. The kernel of Fig. 2.5 has an orientation of N45°E, and it allows the detection of linear features for that direction. If we apply a set of kernels that cover all the directions on the plane with a given angle discretization (for example every 10° from N0E to N170E) to a given spatial object like the karst depression shown in Fig. 2.2, the resulting function will reach higher values for the directions that show a preferential development. That is, if the feature is circular, all the values of the spatial feature



■ **Fig. 2.1** Digital elevation model of the Sierra de las Nieves massif. In the *upper left corner*, there is its geographic location in southern Spain. The *white circle* represents the location of the karst depression shown in ■ **Fig. 2.2**. The *solid black square* represents the area of ■ **Fig. 2.3**, while the *dashed black square* represents the area of ■ **Fig. 2.4**. The units of the legend are meters



■ **Fig. 2.2** Karst depression (“El Águila” doline) in Sierra de las Nieves karst where the main directions of development can be guessed. The legend is depth from the rim of the depression. The units of the legend are meters

(depth in the case of ■ **Fig. 2.2**) multiplied by the kernel will give the same value because the feature is isotropic. However, when there are preferential directions, the kernel with the same direction as the preferential will give a highest value like in the physical process of resonance. The size of the kernel is fitted to the size of each depression, and the bandwidth of the kernel has been chosen in a trial and error procedure, where several bandwidths

have been tried. If the bandwidth is too broad, some preferential directions will be missed, while if the bandwidth is too narrow, there will be too many preferential directions some of them being unimportant. The same set of kernels can be applied to karst hills and to the terrain itself (i.e., to the DEM). In that case, the bandwidth can be selected in a similar trial and error way, although there is not a characteristic scale for the size of the kernel,

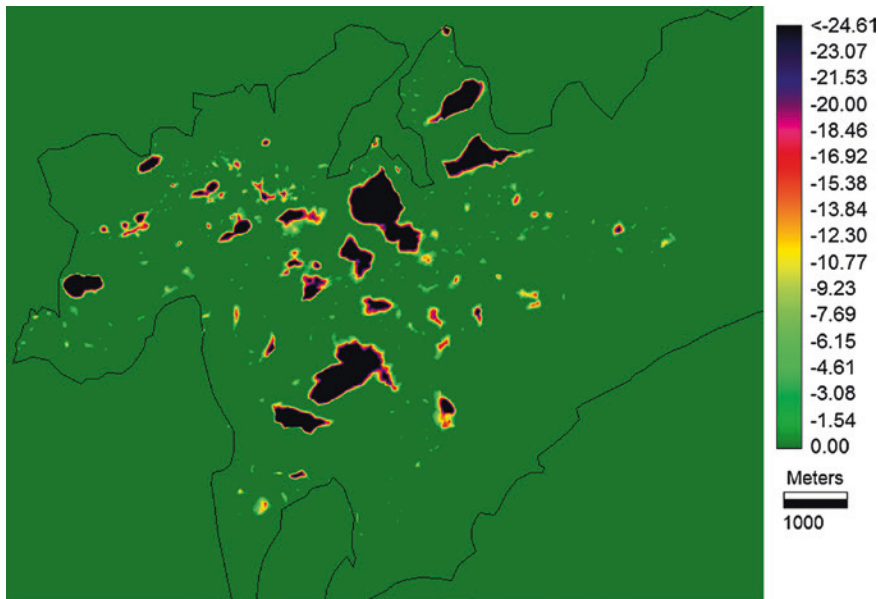


Fig. 2.3 Karst hills that show a spatial pattern clearly controlled by a lineament of fractures. Five hundred ninety-five karst hills have been identified and delineated. This area is shown in **Fig. 2.1** by a black rectangle with solid line, and it corresponds to the downlifted block in relation to the other block

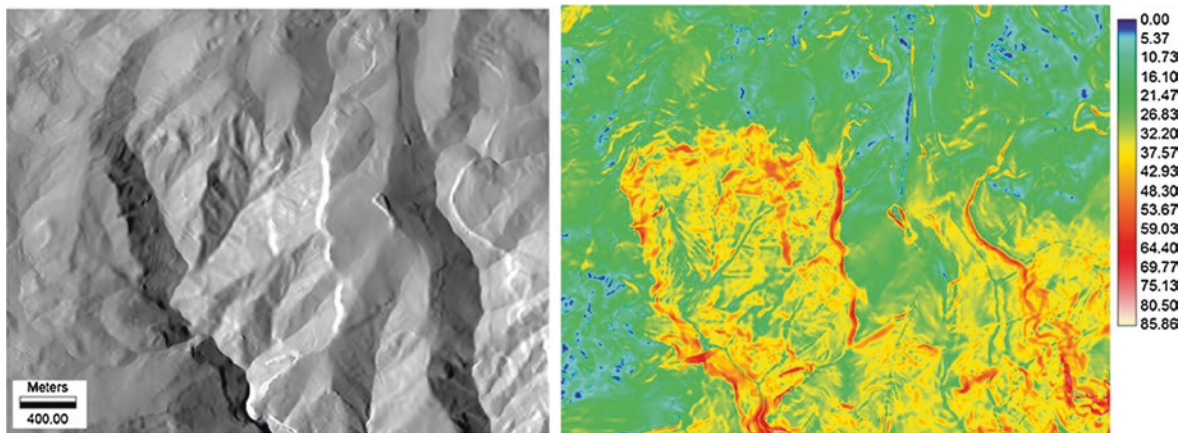


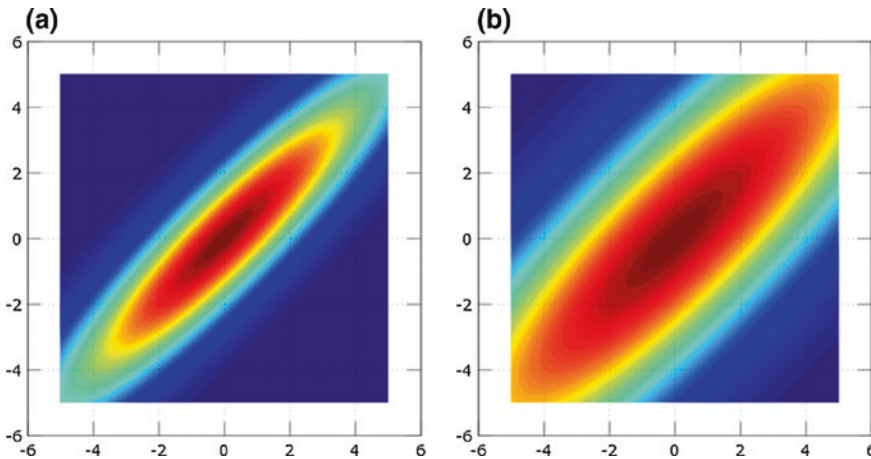
Fig. 2.4 a Shadow map showing the "Turquillas" area (the main fault that divides the two blocks) with the karst scarps (white) that will be the target features of the kernel method. This area is shown for illustrative purpose and it is located in **Fig. 2.1** by a black dashed rectangle. b Slope map (in degree) of the same area as (a)

like in the case of objects. Thus, again several sizes can be tried and the results judged. All this analysis for geomorphic objects and the terrain itself is done in the case study section.

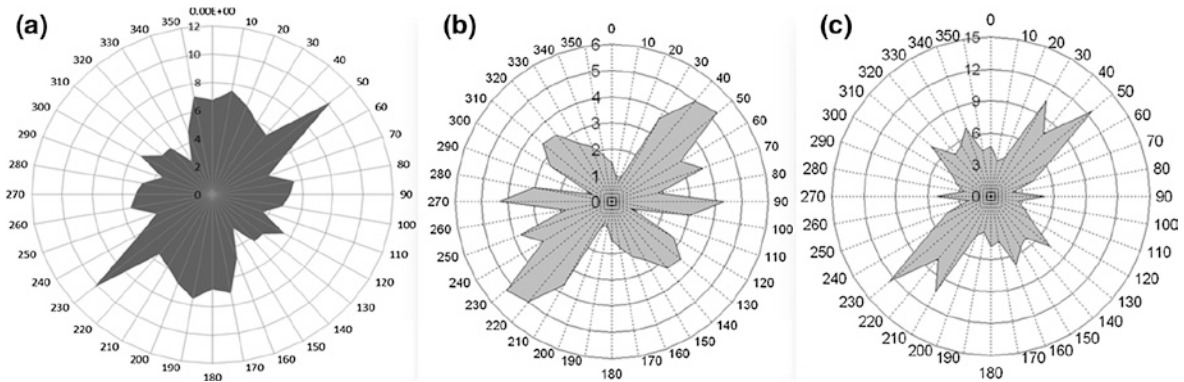
2.3 Case Study

The study area is the Sierra de las Nieves karst aquifer (**Fig. 2.1**) in the province of Málaga, southern Spain (Pardo-Igúzquiza et al. 2015). The area has a ragged orography with an altitude range from 1917 (the highest

altitude of the province) to 450 m a.s.l. that is the altitude of the lowest karst spring. The karst massif consists of a succession of carbonate rock that is folded by an NE–SW trending overturned syncline with a vergency toward the NW. The karst massif is split into two blocks by an important geological fault. One of the blocks has been tectonically uplifted (around 500 m) with respect to the other block. There are three important karst springs and thus three main hydrogeological basins. Each drainage basin has a recharge area which is characterized by a high density of dolines. The results of the kernel analysis for the karst depressions have been shown in



■ **Fig. 2.5** Spatial bivariate Gaussian density function kernels represented with arbitrary units on both axes. This is a kernel for detecting linear features with orientation N45°E. **a** With a narrow bandwidth. **b** With a broad bandwidth



■ **Fig. 2.6** **a** Direction rose of 595 directions of development of karst hills represented in ■ Fig. 2.3. **b** Direction rose of 375 directions of development of karst hills represented in figure. **c** Direction rose of 323 main directions of karst depressions

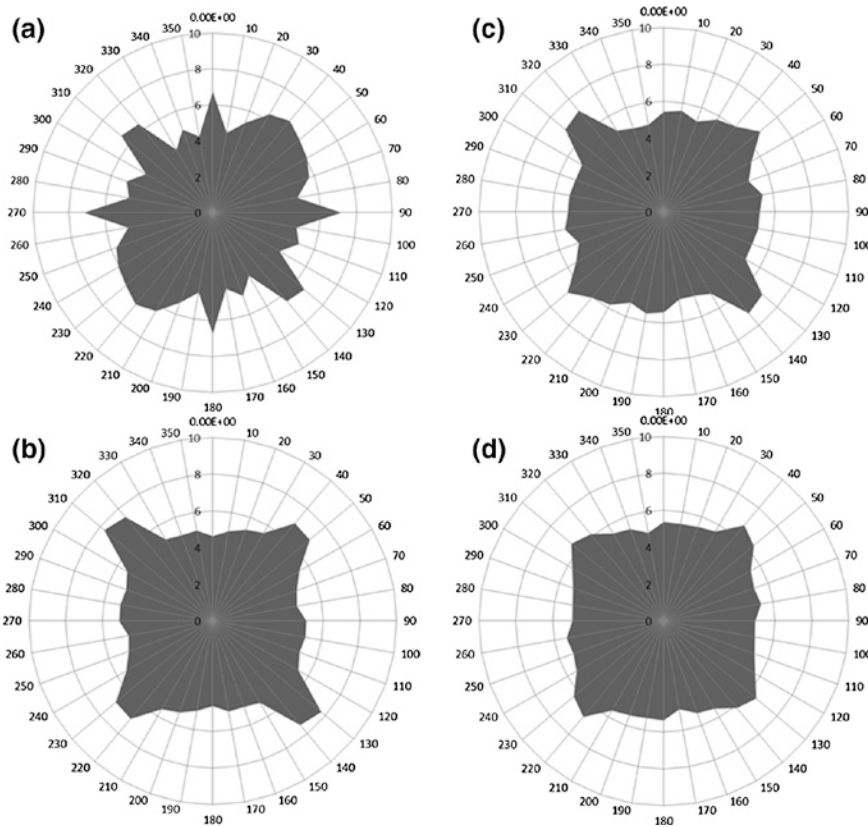
Pardo-Igúzquiza et al. (2013). In that study, it is shown how the main directions of development of depressions are coincidental with the main directions of the geological faults in the area (■ Fig. 2.6b, c). The main directions of the karst hills are shown in ■ Fig. 2.6a. It may be seen how, apart the main directions of the faults, N50E, N90E and N130E, which is coincidental with the principal directions of karst depressions, there is a principal direction of karst hills along the N–S direction because it is the main remaining direction that was not used by the depressions.

In the case of finding the main direction of the terrain itself, the results are shown in ■ Fig. 2.7 for different scales of study. The scales that have been studied are 50 m × 50 m (■ Fig. 2.7a), 150 m × 150 m (■ Fig. 2.7b), 300 m × 300 m (■ Fig. 2.7c) and 500 m × 500 m (■ Fig. 2.7d). For the smallest scale of 50 m × 50 m, all the directions known to be important have been identified. The main directions are N30–60E, then N130–140E

and secondarily the N–S and E–W directions. As the scale of grows, only the modes of the directions N40E and N130E remain. Again, those are the main directions of geological faults.

2.4 Conclusions

The availability of high-resolution models has opened multiple possibilities for the quantitative analysis of terrains in general and the karst landscape in particular. Two of the most distinctive geoforms of a karst relief are karst depressions and terrain scarps. This is particularly true in the Sierra de las Nieves karst massif that is a Mediterranean high-relief karst where there is a combination of multiple depressions in areas of low slope and important scarps in areas with high slope. An adaptive spatial kernel has been designed in order to extract information on principal directions of depressions, karst



■ Fig. 2.7 Direction roses of the terrain for different characteristic scales: **a** 50 m × 50 m. **b** 150 m × 150 m. **c** 300 m × 300 m. **d** 500 m × 500 m

hills and the relief itself. In all the cases, there is a strong structural control by the faults and fractures as well as by the structural disposition of the area (direction of the fold) and the strike of bedding. It is also shown how the main direction of the karst hills is the N–S which is the one that is left by the development of the depressions.

Acknowledgments This work was supported by the research project CGL2015-71510-R from the Ministerio de Economía y Competitividad of Spain. We would like to thank the managers of the Parque Natural de la Sierra de las Nieves for facilitating our research at the park. We would like to thank the reviewers for their constructive criticism.

References

- Bishop, M. P. and Shroder, J. F., 2004: *Geographic Information Science and Mountain Geomorphology*. Springer, Berlin, 491 p.
- Pardo-Igúzquiza E., Durán J.J. and Dowd P.A. 2013: Automatic detection and delineation of karst terrain depressions and its application in geomorphological mapping and morphometric analysis. *Acta Carsologica* 42/1, 17–24.
- Pardo-Igúzquiza, E., Durán, J.J., Luque-Espinar, J.A. y Martos-Rosillo, S., 2014: Analysis of karst terrains using the digital elevation model. Application to the Sierra de las Nieves (province of Málaga). *Boletín Geológico y Minero*, 125, 381–389.
- Pardo-Igúzquiza, E., Durán, J.J., Luque-Espinar, J.A., Robledo-Ardila, P.A., Martos-Rosillo, S., Guardiola-Albert, C., Pedrera, A., 2015. Karst massif susceptibility from rock matrix, fracture and conduit porosities: a case study of the Sierra de las Nieves (Málaga, Spain). *Environmental Earth Sciences*, 74, 7583–7592.
- Shimazaki H. and Shinomoto, S., 2010: Kernel bandwidth optimization in spike rate estimation. *Journal of Computing Neurosciences*, 29, 171–182.
- Strahler A. H. and Strahler, A. N., 1992: *Modern physical geography*. Fourth Edition, John Wiley & Sons, New York, 656 p.

EuroKarst 2016, Neuchâtel

Advances in the Hydrogeology of Karst and Carbonate
Reservoirs

Renard, P.; Bertrand, C. (Eds.)

2017, XII, 370 p. 208 illus., 193 illus. in color.,

Hardcover

ISBN: 978-3-319-45464-1